

Research Paper

Calculation of the Penetration Depth of X-rays in Intact Pharmaceutical Film-Coated Tablets by Microdiffractometry

Hiroyuki Yamada^{1,2} and Raj Suryanarayanan^{1,3}

Received January 20, 2006; accepted May 22, 2006; published online August 12, 2006

Purpose. (i) Develop a method to calculate the penetration depth of X-rays in intact film-coated tablets, and validate it using model bilayer tablets. (ii) Characterize the physical form of drug in intact pharmaceutical film-coated tablets by XRD.

Materials and Methods. An equation for the calculation of the penetration depth of X-rays, as a function of the incident angle, was derived. Model bilayer tablets were prepared to validate the calculation method. The upper layer of the tablets consisted only of microcrystalline cellulose, while the lower layer was a mixture of cerium oxide (10% w/w), blue dye (5% w/w) and microcrystalline cellulose. The total tablet thickness was 3,500 μm , with the upper layer thickness ranging from 200 to 700 μm . The diffracted intensity of a cerium oxide peak in the lower layer was determined using a microdiffractometer system (CuK α radiation) with a two-dimensional area detector. The calculated penetration depth of X-rays was compared with that determined by XRD. After validation of the XRD method, commercial ibuprofen tablets were characterized.

Results. The penetration depth calculated by the method developed in this study was, in general, in good agreement with that determined experimentally by XRD. In commercial ibuprofen tablets, the coating material exhibited peaks due to TiO₂ (25.4°2 θ) and Fe₂O₃ (33.3°). However, these did not interfere with the characteristic peak of ibuprofen (22.2°).

Conclusion. We developed a method for calculation of penetration depth of X-rays in film-coated tablets and validated it using the model bilayer tablets. This method enables the characterization of the active pharmaceutical ingredient in different regions (at different depths) of the film-coated tablet. Since the technique is nondestructive, the same tablet can be repeatedly analyzed during stability studies.

KEY WORDS: film-coated tablet; microdiffractometry; penetration depth; physical form; X-ray.

INTRODUCTION

The performance, stability and effectiveness of a solid dosage form of the pharmaceutical drug can be influenced by the physical form of the active pharmaceutical ingredient (API). Although the physical form of an API may be carefully selected for dosage form manufacture, the processing conditions will determine the solid state of the drug in the final product. The processing steps during tablet manufacture may include milling, granulation, drying, compression and coating. In addition to particle size reduction, milling is also known to cause a decrease in the degree of crystallinity (1). Tablet compression has resulted in polymorphic transformations in several drugs including chlorpropamide (2) and carbamazepine (3). The use of a binder solution for wet granulation can cause solvent-mediated phase transformations. For example, during aqueous wet granulation, the

stable theophylline anhydrate polymorph was converted to theophylline monohydrate, which interestingly dehydrated to a metastable anhydrate during drying (4). We have also recently demonstrated that phase transformations during dissolution can influence the observed dissolution rates (5).

X-ray powder diffractometry is recognized as a powerful tool for physical characterization of pharmaceutical solids (6). The technique has also been used to quantify the drug content in tablets and also to monitor the kinetics of solid-state reactions (7–10). Recently a glancing angle XRD technique was developed to profile phase transformations as a function of tablet depth in uncoated tablets (11). This technique was then used to study both drug crystallization and anhydrate \rightarrow hydrate transformations during tablet dissolution. Several recent advances in instrumentation, such as the parallel beam geometry, and advances in software, such as pattern fitting, have facilitated analyses of intact tablets (12,13).

A significant fraction of commercially available tablets are film-coated, wherein the tablet surface is coated with a thin layer of a polymeric material. The characterization of intact film-coated tablets, by X-ray diffractometry, poses some unique challenges. The coating film will be substantial or completely amorphous, depending on the nature of the

¹Department of Pharmaceutics, University of Minnesota, 308 Harvard Street, SE Minneapolis, Minnesota 55455, USA.

²Pharmaceutical Development Laboratory, Mitsubishi Pharma Corporation, 14 Sunayama, Kamisu, Ibaraki 314-0255, Japan.

³To whom correspondence should be addressed. (e-mail: surya001@umn.edu)

coating material. In addition to attenuating the intensity of the diffracted radiation, the XRD pattern of the film-coating may interfere with that of the API. Since the depth of penetration of X-rays is a function of the incident angle, it is possible to perform phase characterization, at different depths from the surface (14,15). Such an approach has been used to analyze the residual stress and strain as a function of depth in thin semiconductor films and also for phase identification in multicomponent thin films (16,17).

Microdiffractometers, with two-dimensional area detectors, are commercially available (18,19). The X-ray beam is focused in a small sample area and the two-dimensional detector allows quick data acquisition as a “snap-shot” over a wide angular range. There are no constraints with regard to sample shape and intact tablets, in a variety of shapes and sizes, can be analyzed directly. There is the potential to monitor phase composition as a function of tablet depth by varying the incident angle.

Our overall objective was to develop a technique to characterize the physical form of the API in intact film-coated tablets. As a first step, model bilayer tablets were used to experimentally determine the depth of penetration of X-rays as a function of the incident angle. This method was validated and then used to characterize commercial film-coated ibuprofen tablets.

THEORY

The change in the diffracted intensity, I_D , as a function of the depth of the powder bed, x , in a powder bed of length l , can be expressed by Eq. (1) (20);

$$dI_D = I_0 a b e^{-\mu x \left(\frac{1}{\sin \gamma} + \frac{1}{\sin \beta} \right)} dx \quad (1)$$

where I_0 is the incident beam intensity, a is the volume fraction of the specimen particles correctly oriented for diffraction, b is the fraction of the incident radiation diffracted by unit sample volume, μ is the linear attenuation coefficient of the sample, γ is the angle between the X-ray beam and the specimen, and β is the angle between the diffracted beam and the specimen. We will initially consider the uncoated, i.e., core tablet. In the geometry shown in Fig. 1a, $\gamma = \Omega$, $\beta = 2\theta - \Omega$, $\mu = \mu_{\text{core}}$ (the linear attenuation coefficient of the core tablet) and the product of a , b and l can be regarded as a constant, K , for a given angle, Ω . Therefore the diffracted intensity from the core tablet is given by:

$$dI_{D\text{core}} = I_0 K e^{-\mu_{\text{core}} x \left(\frac{1}{\sin \Omega} + \frac{1}{\sin(2\theta - \Omega)} \right)} dx \quad (2)$$

The total diffraction intensity, $I_{D\text{core}}$, is obtained by integrating Eq. (2) from the surface, i.e., $x = 0$, to a depth of c , the maximum depth from which diffracted X-rays reached the detector.

$$I_{D\text{core}} = I_0 K \left\{ \frac{- \left[e^{-\mu_{\text{core}} c \left(\frac{1}{\sin \Omega} + \frac{1}{\sin(2\theta - \Omega)} \right)} - 1 \right]}{\mu_{\text{core}} \left[\frac{1}{\sin \Omega} + \frac{1}{\sin(2\theta - \Omega)} \right]} \right\} \quad (3)$$

In the film-coated tablet (Fig. 1b), with a coating of thickness f , the incident X-ray intensity decreases due to the absorption by the film coating material before reaching the core tablet by a factor of $\exp(-\mu_{\text{film}} f / \sin \Omega)$, where μ_{film} is the linear attenuation coefficient of the coating. Similarly, the diffracted radiation is attenuated by a factor of $\exp[-\mu_{\text{film}} f / \sin(2\theta - \Omega)]$, since it has a path length of $f / \sin(2\theta - \Omega)$ in the coating film. Thus, the peak intensity from the core of the film-coated tablet, $I_{D\text{coated}}$, is expressed by Eq. (4).

$$dI_{D\text{coated}} = I_0 e^{-\mu_{\text{film}} f \left(\frac{1}{\sin \Omega} \right)} \left[K e^{-\mu_{\text{core}} x \left(\frac{1}{\sin \Omega} + \frac{1}{\sin(2\theta - \Omega)} \right)} dx \right] e^{-\mu_{\text{film}} f \left(\frac{1}{\sin(2\theta - \Omega)} \right)} \quad (4)$$

The total diffracted intensity is obtained by integrating Eq. (4) from 0 to d , where d is the maximum depth in the core (of a film-coated tablet) from which diffracted X-rays reached the detector.

$$I_{D\text{coated}} = I_0 K e^{-\mu_{\text{film}} f \left(\frac{1}{\sin \Omega} + \frac{1}{\sin(2\theta - \Omega)} \right)} \times \left\{ \frac{- \left[e^{-\mu_{\text{core}} d \left(\frac{1}{\sin \Omega} + \frac{1}{\sin(2\theta - \Omega)} \right)} - 1 \right]}{\mu_{\text{core}} \left[\frac{1}{\sin \Omega} + \frac{1}{\sin(2\theta - \Omega)} \right]} \right\} \quad (5)$$

Equation (6) is obtained by dividing Eq. (5) by Eq. (3).

$$\frac{I_{D\text{coated}}}{I_{D\text{core}}} = \frac{e^{-\mu_{\text{film}} f \left(\frac{1}{\sin \Omega} + \frac{1}{\sin(2\theta - \Omega)} \right)} \times \left\{ e^{-\mu_{\text{core}} d \left(\frac{1}{\sin \Omega} + \frac{1}{\sin(2\theta - \Omega)} \right)} - 1 \right\}}{e^{-\mu_{\text{core}} c \left(\frac{1}{\sin \Omega} + \frac{1}{\sin(2\theta - \Omega)} \right)} - 1} \quad (6)$$

In Eq. (2), we had expressed the intensity of radiation diffracted from the uncoated (i.e., only core) tablet, when the

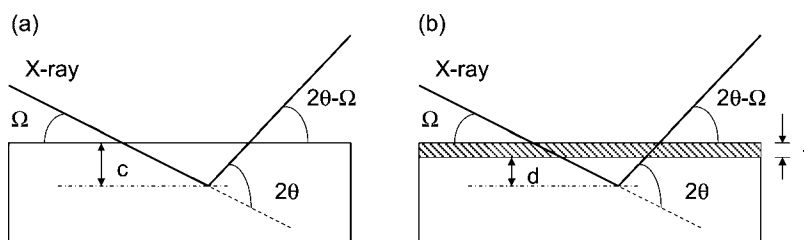


Fig. 1. Schematic representation of diffraction of X-rays through an (a) uncoated and (b) film-coated tablet.

penetration depth was x . When the penetration depth is c , the equation is modified to:

$$dI_{D_{\text{core}}} = I_0 K e^{-\mu_{\text{core}} c \left(\frac{1}{\sin \Omega} + \frac{1}{\sin(2\theta - \Omega)} \right)} dx \quad (7)$$

Similarly, the diffracted intensity from depth d for the film-coated tablet is obtained by modification of Eq. (4) to yield Eq. (8)

$$dI_{D_{\text{coated}}} = I_0 e^{-\mu_{\text{film}} f \left(\frac{1}{\sin \Omega} \right)} \left[K e^{-\mu_{\text{core}} d \left(\frac{1}{\sin \Omega} + \frac{1}{\sin(2\theta - \Omega)} \right)} dx \right] e^{-\mu_{\text{film}} f \left(\frac{1}{\sin(2\theta - \Omega)} \right)} \quad (8)$$

Since c and d are the maximum depths from which diffracted X-rays reached the detector in core and coated tablets, respectively, and Eqs. (7) and (8) express the respective minimum detectable diffracted intensity from the core and coated tablets, Eq. (7) = Eq. (8).

Therefore,

$$\mu_{\text{core}} c = \mu_{\text{film}} f + \mu_{\text{core}} d \quad (9)$$

Substituting Eq. (9) in Eq. (6), and solving for d yields;

$$d = \ln \left[\frac{e^{-\mu_{\text{film}} f \left(\frac{1}{\sin \Omega} + \frac{1}{\sin(2\theta - \Omega)} \right)} - \frac{I_{D_{\text{coated}}}}{I_{D_{\text{core}}}}}{e^{-\mu_{\text{film}} f \left(\frac{1}{\sin \Omega} + \frac{1}{\sin(2\theta - \Omega)} \right)} \left(1 - \frac{I_{D_{\text{coated}}}}{I_{D_{\text{core}}}} \right)} \right] \left/ \left[-\mu_{\text{core}} \left(\frac{1}{\sin \Omega} + \frac{1}{\sin(2\theta - \Omega)} \right) \right] \right. \quad (10)$$

If μ_{film} , μ_{core} and f (thickness of film coating) are known, the penetration depth, d , can be calculated using the diffracted peak intensities ($I_{D_{\text{core}}}$ and $I_{D_{\text{coated}}}$) and Eq. (10).

In most situations, the physical form of the API will be of interest and therefore a characteristic peak of the API will form the basis for tablet characterization. However, the approach is equally valid for any crystalline formulation component.

MATERIALS AND METHODS

Materials

Microcrystalline cellulose (Avicel® PH-101, FMC, Philadelphia, PA, USA), cerium oxide (Standard Reference Material 674a, National Institute of Standards and Technology (NIST), Gaithersburg, MD, USA), blue dye (Brilliant Blue FCF, San-Ei Chemical Industries, Osaka, Japan) were used as received. Ibuprofen tablets (film-coated tablets containing 200 mg ibuprofen per tablet (total tablet weight of 325 mg), Supervalu Inc., Eden Prairie, MN, USA) were purchased in a local pharmacy.

Model Bilayer Tablets

In an effort to simulate the film-coated tablets, model bilayer tablets were prepared, with the upper layer representing the coating film, and the lower layer, the tablet core. The lower layer was first compressed, and the powder constituting the upper layer was added on top, and the system compressed

again. The lower layer contained cerium oxide (10% w/w), blue dye (5% w/w) and microcrystalline cellulose (85% w/w). Table I contains the tablet compositions. Appropriate amount of powder (280 to 330 mg) was filled in a circular stainless steel holder (10 mm internal diameter) and compressed in a hydraulic press (Carver Model C Laboratory press, Menomonee Falls, WI, USA) to 125 MPa for 1 min. Appropriate amount of microcrystalline cellulose (up to 70 mg) was added to the top of the tablet and compressed again to 125 MPa for 1 min, to yield the bilayer tablet. The die and punch assembly yielded tablets with a thickness of 3.5 mm. By maintaining the total tablet weight (lower + upper layer) at 350 mg, it was also possible to control the thickness of the upper layer. Typically, each 10 mg of microcrystalline cellulose conferred a thickness of 100 μm to the upper layer. Tablets with desired upper layer thickness of 200 to 700 μm were prepared. The blue color of the lower layer, conferred by the dye, enabled clear demarcation between the lower and upper layers and enabled the optical measurement of the upper layer thickness. The thickness of the upper layer was measured using an optical microscope (Table I). The cerium oxide, added to the lower layer, was characterized by several intense diffraction lines (21). The line with d-spacing of 3.12 \AA ($28.6^\circ 2\theta$; CuK α radiation) was used to determine the depth of penetration of X-rays. Cerium oxide did not undergo any detectable physical transformations at compression pressure of 125 MPa.

Microdiffractometry

A microdiffractometer XRD system with a two-dimensional area detector (D8 DISCOVER, Bruker AXS) was used, wherein X-rays (CuK α radiation; 45 kV \times 40 mA) were collimated to 0.8 mm i.d. spot size. In order to vary the depth of penetration of X-rays, the incident angle (Ω) ranged from 5 to either 15.0° (bilayer tablet) or 17.5° (ibuprofen tablet) with a step size of 2.5° . The data was collected for 180 s at each step. The detector position was fixed at $25^\circ 2\theta$, which covered the angular range from 10 to $40^\circ 2\theta$. The results were analyzed using commercially available software (JADE, Materials Data, Inc, Livermore, CA, USA).

Scanning Electron Microscopy

In order to determine the thickness of the coating film, the ibuprofen tablet was transversely sliced with a razor

Table I. Composition of Model Bilayer Tablets and the Thickness of the Upper Layer

Weight (mg)		Upper layer thickness (μm)	
Upper layer	Lower layer	Desired (μm)	Measured (μm)*
20	330	200	202 \pm 10
30	320	300	297 \pm 7
40	310	400	395 \pm 8
50	300	500	493 \pm 7
60	290	600	589 \pm 7
70	280	700	687 \pm 8

*mean \pm S.D; $n = 10$.

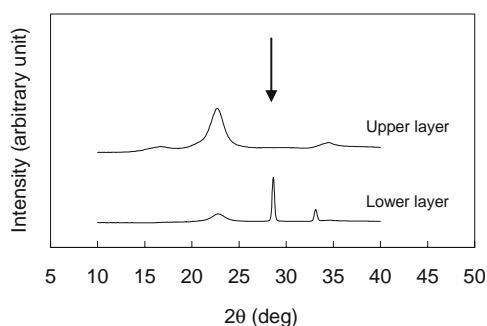


Fig. 2. Microdiffraction patterns of the upper layer (microcrystalline cellulose) and the lower layer (microcrystalline cellulose, cerium oxide and blue dye) of tablets. Special tablets consisting only of the upper layer and the lower layer materials were prepared for this purpose. The incident angle (Ω) was 15.0° .

blade, mounted on the sample holder with double sided carbon tape, coated with platinum (50 \AA) and observed under an electron microscope (Model: JSM-6500F, JEOL, Tokyo, Japan).

Elemental Analysis

In the ibuprofen tablets, the film coating was manually separated from the core tablet. The elemental composition of both the core tablet and the coating material were determined. The C, H and N content were directly determined (2400 Series II CHN Analyzer, Perkin Elmer, Wellesley, MA, USA; calibrated with an acetanilide). The Si, Na, Ti and Fe content was determined spectroscopically after appropriate sample preparation (JY38S ICP-AES spectrometer, Jobin Yvon, Longjumeau, France).

RESULTS AND DISCUSSION

Depth of Penetration of X-rays in Model Bilayer Tablets

Equation (10) provides the penetration depth (d) of X-rays as a function of the incident angle (Ω). It is evident that in film-coated tablets, the penetration depth will depend on the mass attenuation coefficients of the core and coating material. In order to experimentally verify Eq. (10), model

bilayer tablets of known composition and coating thickness were prepared. The depth of penetration calculated using Eq. (10) was compared with that obtained experimentally by XRD. Since the coating (upper layer) thickness in the model bilayer tablets was directly determined by optical microscopy, it was possible to check the validity of the XRD results.

In the model bilayer tablets, as described in the Experimental section, the lower layer contained cerium oxide, blue dye and microcrystalline cellulose, while the upper layer consisted only of microcrystalline cellulose. As shown in Fig. 2, while the upper layer is characterized by the amorphous halo of microcrystalline cellulose, the lower layer exhibited an intense diffraction peak of cerium oxide at a 2θ value of 28.6° . In order for the characteristic $28.6^\circ 2\theta$ peak of cerium oxide to be detected, it is necessary for the X-rays to completely penetrate the upper layer. This peak formed the basis for the determination of the penetration depth of X-ray in the bilayer tablets.

Calculation of the Penetration Depth

In order to calculate the depth of penetration of X-rays at a given incident angle Eq. (10), the linear attenuation coefficient values of the lower and upper layers should be known. However, in the literature, only the mass attenuation coefficients of elements are available (20). The mass attenuation coefficient of a compound is the weighted average of the mass attenuation coefficients of the constituent elements. The mass attenuation coefficient of a powder mixture can be calculated based on the weight fraction of the components and their elemental compositions. The mass attenuation coefficient, multiplied by the density, yielded the linear attenuation coefficient. These determined values, and the basis of the determination are summarized in Table II.

We will first explain the method for calculating the value of d (depth of X-ray penetration in the core region of the bilayer tablet, Eq. (10)) in model bilayer tablets, wherein the upper layer (microcrystalline cellulose) thickness is $202 \mu\text{m}$. At chosen Ω values, the integrated intensity (peak area) of the $28.6^\circ 2\theta$ peak of cerium oxide in the bilayer tablet was experimentally determined ($I_{D\text{coated}}$). Similarly, $I_{D\text{core}}$ is the experimentally determined intensity of the $28.6^\circ 2\theta$ peak of cerium oxide in the core (i.e., consisting only of the lower layer) tablet. Based on the known values of the linear attenuation coefficients (μ ; Table II), d can then be calculat-

Table II. Attenuation Coefficient and Density Values of the Upper and Lower Layers of the Model Bilayer Tablets

Property	Determined value	Basis of determination
Mass attenuation coefficient of upper layer $[(\mu/\rho)_{\text{upper}}]$	$7.34 \text{ cm}^2/\text{g}$	Calculated from the chemical composition and mass attenuation coefficients of the constituent elements
Mass attenuation coefficient of lower layer $[(\mu/\rho)_{\text{lower}}]$	$37.87 \text{ cm}^2/\text{g}$	Determined from the weight and volume of the upper and lower tablet layer
Density of upper layer $[\rho_{\text{upper}}]$	$1.274 \text{ g}/\text{cm}^3$	
Density of lower layer $[\rho_{\text{lower}}]$	$1.274 \text{ g}/\text{cm}^3$	Calculated from the relationship: Linear attenuation coefficient = mass attenuation coefficient \times density
Linear attenuation coefficient of upper layer $[\mu_{\text{upper}}]^*$	9.4 cm^{-1}	
Linear attenuation coefficient of lower layer $[\mu_{\text{lower}}]**$	48.2 cm^{-1}	
Thickness of the upper layer $[f]$	0.0202 cm	Determined by optical microscopy

*This is referred to as μ_{film} in the Theory section.

**This is referred to as μ_{core} in the Theory section.

Table III. Penetration Depth of X-rays as a Function of the Incident Angle (Ω)

Ω (degree)	Penetration depth (μm)	
	Calculated (\pm S.D., $n = 3$)*	Measured**
5.0	395 \pm 18	339–437
7.5	490 \pm 19	440–538
10.0	538 \pm 20	534–630
12.5	570 \pm 14	540–636
15.0	638 \pm 39	665–763

The ‘calculated’ values were obtained using Eq. (10) and the experimentally determined values of $I_{D_{\text{core}}}$ and $I_{D_{\text{coated}}}$. The ‘measured’ values were based on the detection of the $28.6^\circ 2\theta$ peak of cerium oxide.

*Using model bilayer tablets with an upper layer thickness of 202 μm .

**Using model bilayer tablets with upper layer thicknesses ranging from 202 to 687 μm .

ed using Eq. (10) (Fig. 1b). Since our interest is to determine the depth of penetration in the upper layer of the model bilayer tablet, it was necessary to convert the value of d to an equivalent penetration depth in the upper layer. This conversion factor was $\mu_{\text{lower}}/\mu_{\text{upper}}$, where μ_{lower} and μ_{upper} are the linear attenuation coefficients of the lower and upper layers, respectively. Therefore the calculated depth of penetration through the lower layer, d , can be converted to equivalent penetration depth in the upper layer through the term: $(d \frac{\mu_{\text{lower}}}{\mu_{\text{upper}}})$. Thus the total depth of penetration (in μm), assuming that the tablet is made up only of the upper layer material (i.e., microcrystalline cellulose), can be expressed as: $(d \frac{\mu_{\text{lower}}}{\mu_{\text{upper}}} + 202)$, since the upper layer thickness in the model bilayer tablet was 202 μm . These calculated values, assuming that the tablet is made up only of microcrystalline cellulose, are given under the column entitled, ‘Calculated’ in Table III.

Determination of the Penetration Depth by XRD and Microscopy

Model bilayer tablets, with upper layer thickness ranging from 202 to 687 μm , were used to determine the penetration depth of X-rays (Table I). The upper layer thickness in these cases was measured with an optical microscope.

The penetration depth of X-rays can be experimentally determined, based on the observed XRD patterns of the model bilayer tablets. If the characteristic peaks of cerium oxide, which is contained only in the lower layer, are discernible, then the X-rays must have completely penetrated through the upper layer so as to reach the lower layer. As mentioned earlier, the intense peak of cerium oxide at $28.6^\circ 2\theta$ was used for this purpose. The depth of penetration was determined using tablets which differed in their upper layer thickness by ~ 100 μm (Table I). Our method therefore does not provide a single value for the penetration depth. Instead, we obtain the higher and lower limits of the depth of penetration. In other words, the depth of penetration is expressed as a range. Profiles (B) and (C) in Fig. 3a, respectively, yielded the lower and higher limits of the depth of penetration. At $\Omega = 5.0^\circ$ (Fig. 3a), the $28.6^\circ 2\theta$ diffraction peak of cerium oxide was detected (indicated by the arrow)

in the XRD pattern of the model bilayer tablet with upper layer thickness values of 202 and 297 μm , but not detected in tablets with an upper layer thickness of 395 μm . Therefore, as a crude but first approximation, the penetration depth can be estimated to be between 297 and 395 μm .

The peak at $28.6^\circ 2\theta$ is due to diffraction from the (111) plane of cerium oxide (21). In order for this to be detectable, diffraction through numerous (111) planes will have to occur. The minimum thickness of the cerium oxide layer through which diffraction will have to occur to yield a detectable signal (hereafter referred to as Δd) was calculated using Eq. (5) after appropriate modification (details in Appendix). At $\Omega = 5.0^\circ$, Δd was calculated to be 8.3 μm . This can be converted to equivalent penetration depth in the upper layer material through the term: $(\Delta d \frac{\mu_{\text{lower}}}{\mu_{\text{upper}}})$, and was calculated to be 42 μm .

Using profile B in Fig. 3a as an example, we will discuss the results. The $28.6^\circ 2\theta$ peak of cerium oxide was detected when the thickness of the upper layer was 297 μm . We will assume that, at this thickness, the diffraction from the $28.6^\circ 2\theta$ peak of cerium oxide is just above the limit of detection. Therefore the calculated total depth of penetration, assuming that the tablet is made up only of the upper

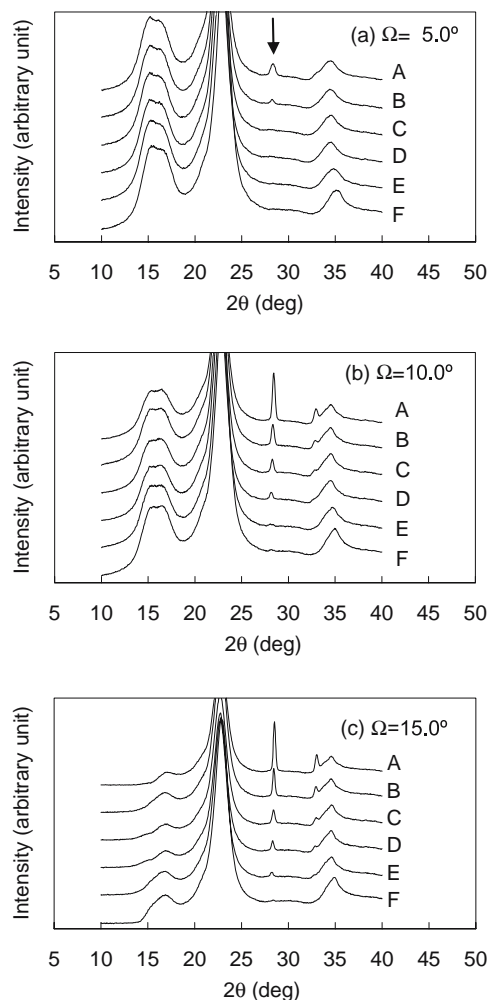


Fig. 3. Microdiffraction patterns of model bilayer tablets with various upper layer thicknesses (A 202 μm , B 297 μm , C 395 μm , D 493 μm , E 589 μm , F 687 μm). The incident angle (Ω) was (a) 5.0, (b) 10.0, and (c) 15.0°.

layer material (i.e., microcrystalline cellulose), can be expressed as: $(297 + \Delta d \frac{\mu_{\text{lower}}}{\mu_{\text{upper}}})$, and was calculated to be 339 μm (Table III; column entitled, 'Measured'). This calculated value forms the lower limit of the depth of penetration of the upper layer at $\Omega = 5.0^\circ$. In other words, the X-rays will penetrate *at least* to a depth of 339 μm through the upper layer material (i.e., microcrystalline cellulose) at $\Omega = 5.0^\circ$.

Our next object is determine the higher limit of the depth of penetration of X-rays at $\Omega = 5.0^\circ$. The $28.6^\circ 2\theta$ peak of cerium oxide is absent when the thickness of the upper layer was 395 μm [profile (C) of Fig. 3a]. We will assume that, at this thickness, the diffraction from the $28.6^\circ 2\theta$ peak of cerium oxide is just below the limit of detection. Using the approach described in the previous paragraph, the calculated total depth of penetration, assuming that the tablet is made up only of the upper layer material (i.e., microcrystalline cellulose), can be expressed as: $(395 + \Delta d \frac{\mu_{\text{lower}}}{\mu_{\text{upper}}})$, and was calculated to be 437 μm (Table III; column entitled, 'Measured'). This calculated value forms the *higher limit* of the depth of penetration of the upper layer at $\Omega = 5.0^\circ$. In other words, the X-rays will penetrate *at most* to a depth of 437 μm through the upper layer material (i.e., microcrystalline cellulose) at $\Omega = 5.0^\circ$.

Figure 3b and c contain the XRD patterns of the tablets obtained with $\Omega = 10.0$ and 15.0° , respectively. It is evident that the depth of penetration of X-rays is a function of their incident angle.

Method Validation

Using the same approach, the penetration depth was calculated and measured at Ω values ranging from 7.5 to 15.0° (Table III). In all these cases, for the purpose of obtaining the 'calculated' values, tablets of a fixed upper layer thickness of 202 μm were used. On the other hand, for obtaining the 'measured' values, tablets of upper layer thickness ranging from 202 to 687 μm were used. At all Ω values (except $\Omega = 15.0^\circ$), the calculated penetration depth was within the range experimentally determined using tablets of different upper layer thickness. Thus the calculated penetration depth in the model bilayer tablets, based on the attenuation coefficients of the coating and the core were, in general, in good agreement with those measured both by microscopy and by XRD.

Microabsorption

The magnitude of absorption of X-rays in the tablets will depend not only on the spatial distribution of the particles of microcrystalline cellulose and cerium oxide but also on their linear attenuation coefficient values (22). The linear attenuation coefficients of microcrystalline cellulose and cerium oxide are 9.4 and 391.7 cm^2/g ($\text{CuK}\alpha$ radiation), respectively. Since their linear attenuation coefficient values are markedly different, microabsorption effects had to be considered. However, microabsorption effects will be negligible when the particle size of both phases is very small. The particles were observed using a scanning electron microscope. While the analyte (cerium oxide) particles were typically <0.5 μm in size, microcrystalline cellulose particles

were <100 μm (longest dimension). In order to determine the effect of particle size, if any, mixtures of cerium oxide (10% w/w), and microcrystalline cellulose (90% w/w) were prepared. In these mixtures, cerium oxide was used 'as is' or after milling for 15 min in a mortar and pestle. Similarly, the microcrystalline cellulose was also used, both before and after milling. The microcrystalline cellulose particles after milling were typically <50 μm (longest dimension). The effect of milling, on the particle size of cerium oxide, was much less pronounced, though the effect was not quantified. In all cases the intensity of the $28.6^\circ 2\theta$ peak of cerium oxide was determined. The integrated intensity was $7,257 \pm 77$ (mean \pm SD; $n = 3$) counts when both the cerium oxide and MCC were unmilled. When only cerium oxide was milled the intensity was $7,160 \pm 81$ counts, while milling only MCC resulted in a peak intensity of $7,195 \pm 55$ counts. From these results, we concluded that any change in the particle size of either cerium oxide or microcrystalline cellulose had no significant (paired *t*-test; $\alpha = 0.01$) effect on the peak intensity. Thus the particle size of both MCC and cerium oxide is sufficiently small to not have any pronounced microabsorption effects.

In order to confirm that the microabsorption effects are negligible, the intensity of a second peak of cerium oxide, at $47.5^\circ 2\theta$, was also determined. The integrated intensity value was $3,233 \pm 33$ (mean \pm SD; $n = 3$) counts when both the cerium oxide and MCC were unmilled. When only cerium oxide was milled, the intensity was $3,168 \pm 17$ counts, while milling only MCC resulted in a peak intensity of $3,187 \pm 45$ counts. These results confirmed that microabsorption effects, if any, would be small.

Analysis of Film-Coated Tablet

Our final objective was to characterize the physical form of the API in intact film-coated tablets. Ibuprofen film-coated tablets were used as the model system. In addition to ibuprofen, the tablets contain corn starch, croscarmellose

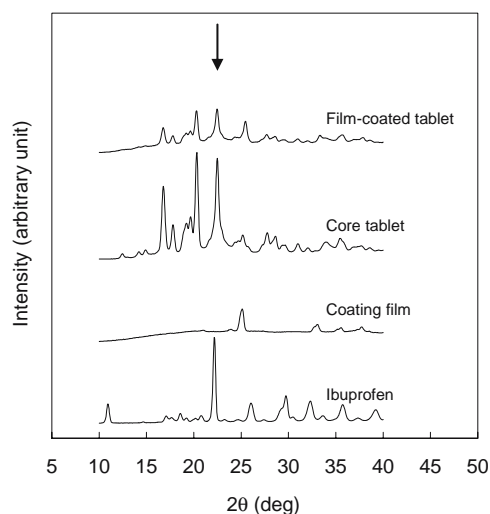


Fig. 4. Microdiffraction patterns of commercially available film-coated ibuprofen tablet. The most intense peak of ibuprofen is pointed out. The diffraction patterns of the core tablet, the coating film, and ibuprofen are also provided for comparison purposes. The incident angle (Ω) was 10.0° .

Table IV. Penetration Depth of X-rays in Film-Coated Ibuprofen Tablets

Ω (degree)	$I_{D_{\text{coated}}}/I_{D_{\text{core}}} (\pm \text{SD}; n = 3)$	Penetration depth (μm) ($\pm \text{SD}; n = 3$)*
5.0	0.153 \pm 0.002	226 \pm 13
7.5	0.225 \pm 0.003	275 \pm 15
10.0	0.273 \pm 0.002	420 \pm 21
12.5	0.257 \pm 0.003	307 \pm 17
15.0	0.197 \pm 0.003	192 \pm 9
17.5	0.124 \pm 0.005	146 \pm 14

*Calculated using Eq. (10) and the experimentally determined values of $I_{D_{\text{core}}}$ and $I_{D_{\text{coated}}}$.

sodium, hypromellose (hydroxypropyl methylcellulose), microcrystalline cellulose, iron oxides, stearic acid, silicon dioxide and titanium dioxide. Unlike highly crystalline materials, the XRD patterns of starch and the celluloses consist of diffuse halos. Some of the ingredients may be present at such low concentration as to be undetectable by XRD.

The API, at different regions in the tablet, was characterized by progressively increasing the penetration depth of the X-rays. The XRD patterns of ibuprofen powder, the coating film (removed from the tablet using adhesive tape), the core tablet (after removing the coating film from the tablet) and the intact film-coated tablet are shown in Fig. 4. The coating film exhibited peaks due to TiO_2 ($25.4^\circ 2\theta$) and Fe_2O_3 ($33.3^\circ 2\theta$), but these did not interfere with the characteristic peak of ibuprofen at $22.2^\circ 2\theta$.

Effect of Incident Angle on the Depth of Penetration

The ibuprofen peak intensity ($22.2^\circ 2\theta$ peak), determined in the core ($I_{D_{\text{core}}}$) and film-coated tablets ($I_{D_{\text{coated}}}$) as a function of Ω , formed the basis for the calculation of the penetration depth (Table IV). Due to pronounced absorption by the coating film, the $I_{D_{\text{coated}}}/I_{D_{\text{core}}}$ values are substantially <1 . As before, Eq. (10) was used to calculate the penetration depths at the various Ω values. The elemental analysis provided the chemical composition of the film coating and the core ibuprofen tablets. The calculated mass attenuation coefficient values, the density and thickness of the coating film and the density of the core are presented in Table V.

As mentioned in the Introduction section, as the incident angle Ω increases, the X-rays penetrate deeper into the

tablet. Even at a low Ω value of 5° , the characteristic peak of ibuprofen was detected, indicating that X-rays passed through the coating film and penetrated the tablet core. With an increase in Ω , the depth of penetration will increase. However, beyond a critical value ($\Omega = \theta$), the diffracted radiation cannot reach the detector since the diffracted radiation from the deeper regions undergo significant attenuation. As a result, the “effective” penetration depth (i.e., ‘ d ’ is the maximum depth in the core from which diffracted X-rays reach the detector as described in Eq. (5) starts to decrease as $\Omega > \theta$. Figure 1 can be helpful in understanding this observation. The path lengths of the incident and diffracted X-rays are $c/\sin\Omega$ and $c/\sin(2\theta - \Omega)$, respectively (Fig. 1). Therefore, the total path length of X-ray, $c[1/\sin\Omega + 1/\sin(2\theta - \Omega)]$, exhibits a minimum at $\Omega = \theta$. The attenuation of X-rays is proportional to the path length by a factor of $\exp\{-\mu c[1/\sin\Omega + 1/\sin(2\theta - \Omega)]\}$, where μ is the linear attenuation coefficient. It is evident that the attenuation of X-rays is minimum at $\Omega = \theta$. In other words, the highest penetration depth is obtained at $\Omega = \theta$. In the case of ibuprofen tablets, the characteristic peak is at $2\theta = 22.2^\circ$. Thus the penetration depth has the highest value when the incident angle, Ω , was set at around 11.1° (Table IV).

Significance

Conventionally, physical characterization of the API in tablet dosage forms is conducted after crushing the tablet, usually into a fine powder. In film-coated tablets, removal of the coating film is also required. We have demonstrated the utility of XRD to characterize the API in intact film-coated tablets. Thus the technique requires no sample treatment whatsoever. Pharmaceutical processing steps such as wet granulation, drying and film coating can cause phase transformation of the API, and this technique has the potential to detect and possibly quantify the physical forms of the API in the final dosage form. The technique also has the potential to provide quantitative information regarding the API phase composition in different regions (i.e., at different depths) of the tablet. Since the technique is nondestructive, the same tablet can be repeatedly analyzed, for example, during conventional or accelerated stability studies. Though our discussion so far has been restricted to the API, similar analyses of crystalline excipients are also possible. While our studies have been restricted to flat-faced tablets, the technique can be extended to tablets with other shapes.

Table V. Attenuation Coefficient and Density Values of the Coating Film and the Core of Ibuprofen Tablets

Property	Determined value	Basis of determination
Mass attenuation coefficient of coating film $[(\mu/\rho)_{\text{film}}]$	44.59 cm^2/g	Calculated from the chemical composition and mass attenuation coefficients of the constituent elements
Mass attenuation coefficient of core tablet $[(\mu/\rho)_{\text{core}}]$	6.019 cm^2/g	Determined from the weight and volume of coating film and core tablet
Density of coating film $[\rho_{\text{film}}]$	1.073 g/cm^3	
Density of core tablet $[\rho_{\text{core}}]$	1.071 g/cm^3	Calculated from the relationship: Linear attenuation coefficient = mass attenuation coefficient \times density
Linear attenuation coefficient of coating film $[\mu_{\text{film}}]$	47.8 cm^{-1}	
Linear attenuation coefficient of core tablet $[\mu_{\text{core}}]$	6.4 cm^{-1}	
Thickness of the coating film $[f]$	0.0025 cm	Determined by scanning electron microscopy

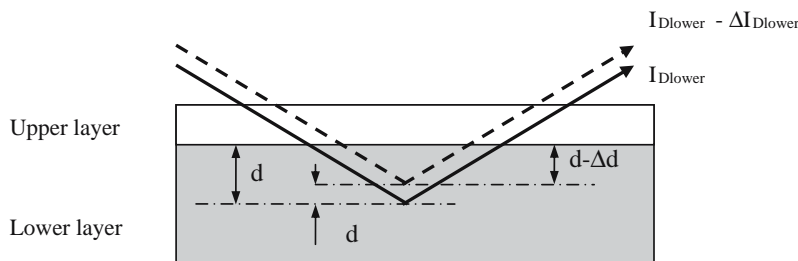


Fig. 1A. Schematic representation of the penetration of X-rays, completely through the upper layer, followed by depth ‘ d ’ through the lower layer. The discontinuous line shows penetration of X-rays through a lower layer, $(d - \Delta d)$, in thickness. Δd is defined as the minimum penetration depth in the lower layer through which diffraction will have to occur to yield a detectable signal (ΔI_{Dlower}).

CONCLUSION

We have developed a method for calculating the penetration of depth of X-rays in film-coated and validated it using model bilayer tablets. The calculated penetration depths were, in general, in good agreement with that determined experimentally, both by XRD and microscopy. In commercial ibuprofen tablets, the coating film exhibited peaks due to TiO_2 ($25.4^\circ 2\theta$) and Fe_2O_3 ($33.3^\circ 2\theta$). However, these did not interfere with the characteristic peak of ibuprofen ($22.2^\circ 2\theta$).

APPENDIX

Minimum penetration depth required for a detectable signal

Equation (5) describes the analyte diffraction intensity from the core in film-coated tablets. This equation has been modified for bilayer tablets [Eq. (A1)], by replacing I_{Dcore} , μ_{film} and μ_{core} with I_{Dlower} , μ_{upper} and μ_{lower} , respectively.

$$I_{Dlower} = I_0 K e^{-\mu_{upper} f \left(\frac{1}{\sin \Omega} + \frac{1}{\sin(2\theta - \Omega)} \right)} \times \left\{ \frac{- \left[e^{-\mu_{lower} d \left(\frac{1}{\sin \Omega} + \frac{1}{\sin(2\theta - \Omega)} \right)} - 1 \right]}{\mu_{lower} \left[\frac{1}{\sin \Omega} + \frac{1}{\sin(2\theta - \Omega)} \right]} \right\} \quad (A1)$$

Similarly, $(I_{Dlower} - \Delta I_{Dlower})$ is obtained by substituting $(d - \Delta d)$ for ‘ d ’ in Eq. (A1) (schematically shown as the discontinuous line in Fig. 1A).

$$I_{Dlower} - \Delta I_{Dlower} = I_0 K e^{-\mu_{upper} f \left(\frac{1}{\sin \Omega} + \frac{1}{\sin(2\theta - \Omega)} \right)} \times \left\{ \frac{- \left[e^{-\mu_{lower} (d - \Delta d) \left(\frac{1}{\sin \Omega} + \frac{1}{\sin(2\theta - \Omega)} \right)} - 1 \right]}{\mu_{lower} \left[\frac{1}{\sin \Omega} + \frac{1}{\sin(2\theta - \Omega)} \right]} \right\} \quad (A2)$$

Equation (A3) is obtained by dividing Eq. (A1) by Eq. (A2).

$$\frac{I_{Dlower}}{I_{Dlower} - \Delta I_{Dlower}} = \frac{e^{-\mu_{lower} d \left(\frac{1}{\sin \Omega} + \frac{1}{\sin(2\theta - \Omega)} \right)} - 1}{e^{-\mu_{lower} (d - \Delta d) \left(\frac{1}{\sin \Omega} + \frac{1}{\sin(2\theta - \Omega)} \right)} - 1} \quad (A3)$$

Solving Eq. (A3) for Δd yields;

$$\Delta d = d - \ln \left[\frac{I_{Dlower}}{I_{Dlower} - \Delta I_{Dlower}} e^{\mu_{lower} d \left(\frac{1}{\sin \Omega} + \frac{1}{\sin(2\theta - \Omega)} \right)} + \frac{\Delta I_{Dlower}}{I_{Dlower}} \right] \left/ \left[-\mu_{lower} \left(\frac{1}{\sin \Omega} + \frac{1}{\sin(2\theta - \Omega)} \right) \right] \right. \quad (A4)$$

The value ‘ ΔI_{Dlower} ’ was determined from the XRD patterns of microcrystalline cellulose tablets containing 0.20, 0.10, 0.05, 0.025 and 0.0125% w/w cerium oxide. The $28.6^\circ 2\theta$ peak of cerium oxide was detected in the tablets containing 0.025% w/w cerium oxide. The signal to noise ratio was 3. Since ‘ I_{Dlower} ’ was experimentally determined and the depth of penetration ‘ d ’ was already calculated by Eq. (10), Δd can be obtained from Eq. (A4).

ACKNOWLEDGMENTS

The financial support of Mitsubishi Pharma Corporation is gratefully acknowledged. We thank Dr. James A. Kaduk (Innovene) for his insightful comments.

REFERENCES

1. R. Lefort, A. De Gussemme, J.-F. Willart, F. Danède, and M. Descamps. Solid state NMR and DSC methods for quantifying the amorphous content in solid dosage forms: an application to ball-milling of trehalose. *Int. J. Pharm.* **280**:209–219 (2004).
2. M. Otsuka, T. Matsumoto, and N. Kaneniwa. Effects of the mechanical energy of multi-tableting compression on the polymorphic transformations of chlorpropamide. *J. Pharm. Pharmacol.* **41**:665–669 (1989).
3. C. Lefebvre, A. M. Guyot-Hermann, M. Draguet-Brughmans, R. Bouché, and J. C. Guyot. Polymorphic transitions of carbamazepine during grinding and compression. *Drug Dev. Ind. Pharm.* **12**:1913–1927 (1986).
4. N. V. Phadnis, and R. Suryanarayanan. Polymorphism in anhydrous theophylline—implications on the dissolution rate of theophylline tablets. *J. Pharm. Sci.* **86**:1256–1263 (1997).

5. S. Debnath, and R. Suryanarayanan. Influence of processing-induced phase transformations on the dissolution of theophylline tablets. *AAPS PharmSciTech*. **5**:1–11 (2003).
6. R. Suryanarayanan. X-ray powder diffractometry. In H.G. Brittain (ed.), *Physical characterization of Pharmaceutical Solids*. Marcel Dekker, New York, 1995, pp. 187–221.
7. R. Suryanarayanan, and C. S. Herman. Quantitative analysis of the active ingredient in a multi-component tablet formulation by powder X-ray diffractometry. *Int. J. Pharm.* **77**:287–295 (1991).
8. V. B. Cooper, G. E. S. Pearce, and C. R. Petts. Quantification of crystalline forms in active pharmaceutical ingredient and tablets by X-ray powder diffraction. *J. Pharm. Pharmacol.* **55**:1323–1329 (2003).
9. S. Rastogi, M. Zakrzewski, and R. Suryanarayanan. Investigation of solid-state reactions using variable temperature X-ray powder diffractometry. I. Aspartame hemihydrate. *Pharm. Res.* **18**:267–273 (2001).
10. S. K. Rastogi, M. Zakrzewski, and R. Suryanarayanan. Investigation of solid-state reactions using variable temperature X-ray powder diffractometry. II. Aminophylline monohydrate. *Pharm. Res.* **19**:1265–1273 (2002).
11. S. Debnath, P. Predecki, and R. Suryanarayanan. Use of glancing angle X-ray powder diffractometry to depth-profile phase transformations during dissolution of indomethacin and theophylline tablets. *Pharm. Res.* **21**:149–159 (2004).
12. W. Cao, S. Bates, G. E. Peck, P. L. D. Wildfong, Z. Qiu, and K. R. Morris. Quantitative determination of polymorphic composition in intact compacts by parallel-beam X-ray powder diffractometry. *J. Pharm. Biomed. Anal.* **30**:1111–1119 (2002).
13. S. Yamamura, and Y. Momose. Quantitative analysis of crystalline pharmaceuticals in powders and tablets by a pattern-fitting procedure using X-ray powder diffraction data. *Int. J. Pharm.* **212**:203–212 (2001).
14. J. Chaudhuri, and S. Shah. Thickness measurement of thin films by X-ray absorption. *J. Appl. Phys.* **69**:499–501 (1991).
15. W. Huaqiang, L. Bin, M. Wei, L. Xingtao, and T. Kun. Computed depth profile method of X-ray diffraction and its application to Ni/Pd films. *Surf. Coat. Technol.* **149**:198–205 (2002).
16. M. F. Doerner, and S. Brennan. Strain distribution in thin aluminum films using X-ray depth profiling. *J. Appl. Phys.* **63**:126–131 (1988).
17. P. Eisenberger, and W. C. Marra. X-ray diffraction study of the germanium (001) reconstructed surface. *Phys. Rev. Lett.* **46**:1081–1084 (1981).
18. B. B. He. Introduction to two-dimensional X-ray diffraction. *Powder Diffr.* **18**:71–85 (2003).
19. B. B. He. Microdiffraction using two-dimensional detectors. *Powder Diffr.* **19**:110–118 (2004).
20. B. D. Cullity, and S. R. Stock. *Elements of X-ray diffraction*, 3rd edn. Prentice Hall, Upper Saddle River, New Jersey, 2001, pp. 630–631.
21. Powder Diffraction File. International Centre for Diffraction Data, Newtown Square, Pennsylvania, 1997, 00-034-0394.
22. H. Hermann, and J. Collazo. Microabsorption of X-ray intensity in fractal microstructures. *J. Appl. Cryst.* **28**:786–792 (1995).